1182

NOVEMBER 1975 MATT-1182

ION-BEAM-DRIVEN RESONANT ION CYCLOTRON INSTABILITY

BY

H. W. HENDEL, M. YAMADA, S. W. SEILER

AND

H. IKEZI

PLASMA PHYSICS LABORATORY

PRINCETON UNIVERSITY
PRINCETON, NEW JERSEY

This work was supported by U. S. Energy Research and Development Administration Contract E(11-1)-3073. Reproduction, translation, publication, use and disposal, in whole or in part, by or for the United States Government is permitted.

NOTICE

Printed in the United States of America.

Available from
National Technical Information Service
U. S. Department of Commerce
5285 Port Royal Road
Springfield, Virginia 22151
Price: Printed Copy $ _*__; Microfiche $1.45

*Pages	NTIS Selling Price
1-50	$ 4.00
51-150	5.45
151-325	7.60
326-500	10.60
501-1000	13.60

Ion-Beam-Driven Resonant Ion Cyclotron Instability

H. W. Hendel,* M. Yamada and S. W. Seiler

Plasma Physics Laboratory, Princeton University
Princeton, New Jersey 08540

and

H. Ikezi

Bell Laboratories, Murray Hill, N. J. 07974

The resonant ion-beam-driven electrostatic ion cyclotron instability is identified. Measured dispersion relation and onset vs. beam energy and density agree with numerical calculations based on a theory which includes beam acoustic terms. After amplitude saturation, velocity space diffusion of the beam ions is observed.

We report experimental results on a resonant, electrostatic ion cyclotron instability destabilized by a low energy ion beam injected parallel to the confining magnetic field into a target plasma. Their interpretation is based on a theory which includes beam acoustic and target ion cyclotron terms and on numerical calculations of the dispersion relation.

Instabilities driven by ion beams have recently attracted considerable interest in connection both with neutral-beam-injection for fusion plasma heating[1] and with space physics.[2] They may scatter particles and waves, effect energy transfer from beam to fusion plasma and vary transport properties of beam and plasma. Ion injection, although differing from neutral injection in time evolution of ion beam density and possibly beam velocity distribution, is easier to set up and should also contribute to the understanding of neutral injection and of the relevant instabilities and their effects on the beam-plasma system. In isothermal ($T_e \approx T_i$) fusion and Q-device plasmas, ion sound is strongly ion Landau damped and not expected to play an important role.[3] However, ion cyclotron waves can have a higher parallel phase velocity and may thus be destabilized more easily by an ion beam with $E_b > kT$.

The significant result of the present work is the detailed identification of the resonant ion-beam-driven electrostatic ion cyclotron wave by measurements of ω and k and of threshold beam energy as function of relative beam density. The experiment is shown to be in agreement with numerical calculations extended from Perkins' theory of counterstreaming beams[4] to include a beam of variable density injected into a plasma at rest. After the wave amplitude saturates, the beam's parallel energy distribution was observed to flatten in the resonant particle region.

The theory considers a uniform, low-β Maxwellian target plasma in a constant uniform magnetic field B, with $T_e = T_{i\perp} = T_o$ and streaming velocity u_t, and an ion beam with streaming velocity u_b and velocity spread characterized by $v_{b\parallel} = \sqrt{\frac{2T_{b\parallel}}{M}}$; $T_{b\perp} = T_o$. The ion beam is injected parallel to B in the z-direction. All species are singly charged so that $n_e = n_{it} + n_{ib}$. The dispersion relation for electrostatic waves propagating almost perpendicularly to B ($k_\perp >> k_z$), for $k_\perp \rho_e << 1 \lesssim k_\perp \rho_i$ is written

$$1 + \frac{k_{De}^2}{k^2} + \frac{k_{Di}^2}{k^2}\left\{\sum_{n=-\infty}^{\infty} I_n(\lambda)e^{-\lambda}\left[1 + \frac{\omega+k_z u_t}{k_z v_i} Z\left(\frac{\omega+k_z u_t+n\omega_{ci}}{k_z v_i}\right)\right]\right\}$$

$$+ \frac{k_{Di}^2}{k^2}\frac{n_{ib}}{n_{it}}\frac{T_i}{T_{b_\parallel}}\left\{\sum_{n=-\infty}^{\infty} I_n(\lambda)e^{-\lambda}\left[1 + \frac{\omega-k_z u_b+n\omega_{ci}\left(1-(T_{b_\parallel}/T_o)\right)}{k_z v_{b_\parallel}}\right.\right.$$

$$\left.\left. Z\left(\frac{\omega-k_z u_b+n\omega_{ci}}{k_z v_{b_\parallel}}\right)\right]\right\} = 0 \qquad (1)$$

where $k_{De(i)}^2 = 4\pi n_{e(it)} e^2/T_o$, $v_i = (2T_o/M)^{1/2}$, $v_{b_\parallel} = (2T_{b_\parallel}/M)^{1/2}$,

and $\lambda = k_\perp^2 T_o/M\omega_{ci}^2$.

$Z(z)$ is the plasma dispersion function and $I_n(\lambda)$ the modified Bessel function of nth order. We note that the parallel beam temperature decreases as $T_{b_\parallel}/T_o \simeq (v_i^2/2u_b^2)$ with increased ion beam energy.[5]

This dispersion relation results in instabilities generated by the interaction between the slow beam-acoustic term and the ion cyclotron mode of the target plasma.[4] Instability occurs when beam-ion inverse Landau damping overcomes target-ion cyclotron damping. Earlier theoretical work on ion beam excited resonant electrostatic ion cyclotron instability[6] used the approximation $\left|\frac{\omega-k_z u_b}{k_z v_{b_\parallel}}\right| > 3$ for the $n = 0$ beam term, discarding instability based on the beam acoustic mode. Since the present experiment covers the regime $\left|\frac{\omega-k_z u_b}{k_z v_{b\parallel}}\right| \simeq 1$, $\left|\frac{\omega+k_z u_t-\omega_{ci}}{k_z v_i}\right| \simeq 1$, we solved Eq. (1) by numerical computation. We note that due to the motion of the target plasma, the cyclotron frequency may be Doppler-shifted ($\omega = \omega_{ci}/2$ for $u_b = u_t$, in the lab-frame), and in addition, cyclotron harmonics may be excited, so that $\omega = n\omega_{ci}(1 - \Delta)$. However, we expect lowest threshold for $\omega = \omega_{ci}(1 - \Delta)$, the wave due to coupling between the beam's slow acoustic and the target plasma's fundamental ion cyclotron modes.

The experiments were performed on the thermally ionized plasma of the Princeton Q-1 device converted into a double-plasma machine,[7,5] Fig. 1. A negatively biased mesh divides the plasma column into a 5 cm long beam-extraction plasma and a 120 cm long target plasma. The plasma diameter is 3.2 cm and the confining magnetic field 2-7 kG. When voltage is applied to the plasma column parallel to B through the ionizer (end) plates, the biased (-20 V) mesh (grid spacing $\lesssim \lambda_{Debye}$) prevents electron flow and the potential drop occurs in the sheath region of the mesh, thus generating an ion beam. Beam and target plasma densities can be varied by regulating the neutral densities impinging on the ionizer plates. Ion collisions are negligible since $\lambda_{mfp} > 10^3$ L (L = machine length). The beam is generally injected on-axis. For the target plasma, $n \simeq 10^9$ cm^{-3}, $T_i \simeq T_e = 0.3$ eV; the relative beam density $n_b/n_t \simeq 0.1 - 5$, and $E_b/E_t = 0 - 10^3$. Probes measure T_e, T_i, n_{it}, n_{ib} (determined with rotating, plane collectors) instability amplitudes and frequencies and their radial profiles. An ion energy analyzer (2 mm diam.) with a 1 mm opening can be turned into beam, target and perpendicular directions and moved radially. Wavelengths are obtained from the phase shift vs. rotation of a double probe $(\lambda_\perp)$ or vs. distance to an axially or radially moving probe $(\lambda_\parallel, \lambda_\perp)$.

Fig. 2a shows measurements of the instability frequency vs. B , for constant u_b , taken well above onset. The observed frequency is below the ion cyclotron frequency, $\omega = \omega_{ci}(1 - \Delta)$, as expected from consideration of the target plasma drift velocity, $\left(\frac{1 - \Delta}{\Delta}\right) \simeq u_b/u_t$. Fig. 2b displays instability frequency vs. ion beam energy, for B = const. At onset, the frequency is about 35% below ω_{ci} , and approaches ω_{ci} as the target-plasma drift becomes negligible relative to the beam velocity, in agreement with the prediction. The resonance coupling between beam and phase velocities is demonstrated in Fig. 2c, which indicates that the phase velocity is about 15% below the beam velocity, in agreement with the computer calculation. For Weibel's[6] purely growing mode $u_b = 2\omega/k_z$, when transformed to the experimental coordinates. We also measured $\lambda_\parallel$ vs. B , for constant beam energy, and found the predicted behavior $\lambda_\parallel \propto 1/\omega_{ci}$. Spatial growth of the wave was observed, with the expected growth rate, converted to temporal growth rate, $\gamma/\omega_{ci} \simeq 0.03$ at maximum. The wave is localized in the interior of the ion beam, with a maximum amplitude $\tilde{n}/n \simeq 15\%$. The radial wavelength was comparable to the beam diameter, so that $k_\perp \rho_i \simeq 1$, as expected.

Fig. 3 shows normalized threshold beam velocity as function of normalized beam density, for constant B. Onset occurs at lowest beam velocity for approximately equal densities of beam and target plasma. We note that two colliding, equal temperature plasmas or beams would produce a symmetrical, parabolic u_b vs. log n_b/n_t plot. If, however, one of the plasmas (the "beam") is reduced in (parallel) temperature (by acceleration), the increased inverse Landau damping leads to an asymmetric plot with lower onset values. Ion-beam-driven ion cyclotron wave results reported previously[8] were limited both experimentally by the set-up and theoretically by the "cold beam-cold plasma" theory used. We also note that a mode at $\omega \simeq 0$ due to coupling of ion-acoustic target and ion cyclotron beam terms at about zero frequency is suggested by Eq. (1). This mode could not be observed because of strong ion Landau damping arising from $T_{it} \simeq T_e$.

Fig. 4 shows parallel energy spread (normalized by the initial value) of the ion-beam as function of beam energy. Since the instability is excited at the expense of parallel ion-beam energy by inverse ion Landau damping, one expects deterioration of the beam energy at the fully developed stage of the instability. At this stage the instability satisfies the qualitative condition for the presence of nonlinear effects ($\omega_{trap.} \simeq \left(\frac{2e\phi}{M} \right)^{1/2} \frac{2\pi}{\lambda_{\parallel}} \simeq k_z v_i \left(\frac{\tilde{n}}{n} \right)^{1/2} \gg \gamma$). The nonlinear wave-particle interactions were observed as flattening (velocity space diffusion) of the beam distribution function on the low energy side where the resonant particles exist, Fig. 4a.

Several important considerations arise from this work. The instability observed here may occur in neutral injection fusion heating. The low threshold values of u_b/u_t measured are due to the reduction of beam parallel temperature with beam acceleration. As the beam density is increased to about 10% of the target plasma density, the instability can be excited, depending on the shape of the distribution function, i.e., transient (narrow beam spread) or steady state (wide spread, small slope) ion beam. Colliding beam tokamaks[9] may be expected to be unstable during the transient switch-on phase (density ratio is one and beam spread narrow) but steady state operation may lead to stable, wide velocity distributions. In linear basic research devices, effects on the target plasma due to beam injection cannot be detected easily, because of the insufficient confinement. However, increased energy transfer from the beam has been demonstrated in this work, which might affect better confined plasmas.

We thank Dr. F. W. Perkins for helpful discussions and Drs. H. P. Eubank, H. P. Furth and T. H. Stix for critical reading of the manuscript.

This work was supported by the U. S. Energy Research and Development Administration (formerly AEC) Contract E(11-1)-3073.

REFERENCES

*On leave from RCA Laboratories, Princeton, New Jersey 08540

[1] T. Stix, Phys. Fluids 16, 1922 (1973); H. L. Berk, et.al., IAEA-CN-33/G2-3, 5th Conf. Plasma Physics and Controlled Nuclear Fusion, Tokyo (1974); B. Coppi, D. K. Bhadra, Phys. Fluids 18, 692 (1975); K. Bol, et.al., Phys. Rev. Lett. 32, 661 (1974); L. A. Berry, et.al., Phys. Rev. Lett. 34, 1085 (1975).

[2] M. D. Montgomery, et.al., Phys. Rev. Lett. 35, 667 (1975).

[3] T. E. Stringer, Plasma Physics 6, 267 (1964); B. D. Fried and A. Y. Wong, Phys. Fluids 9, 1084 (1966).

[4] F. W. Perkins, Princeton Plasma Physics Laboratory MATT-1141 (1975) (submitted to Phys. Fluids).

[5] N. Sato, et.al., Phys. Rev. Lett. 34, 931 (1975).

[6] E. S. Weibel, Phys. Fluids 13, 3003 (1970).

[7] R. J. Taylor, K. R. MacKenzie and H. Ikezi, Rev. Scient. Instr. 43, 1675 (1972).

[8] H. Ishizuka, H. Ono, S. Kojima, J. Phys. Soc. Japan 36, 1158 (1974).

[9] R. M. Kulsrud and D. L. Jassby, Princeton Plasma Physics Laboratory MATT-1114 (1975).

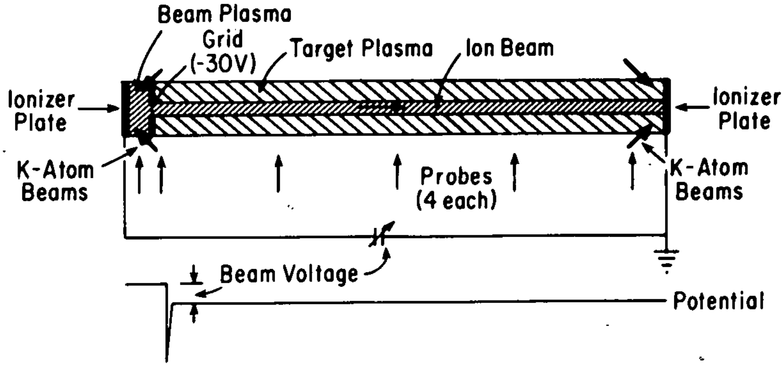

753929

Fig. 1. Diagram of Experimental Set-up.

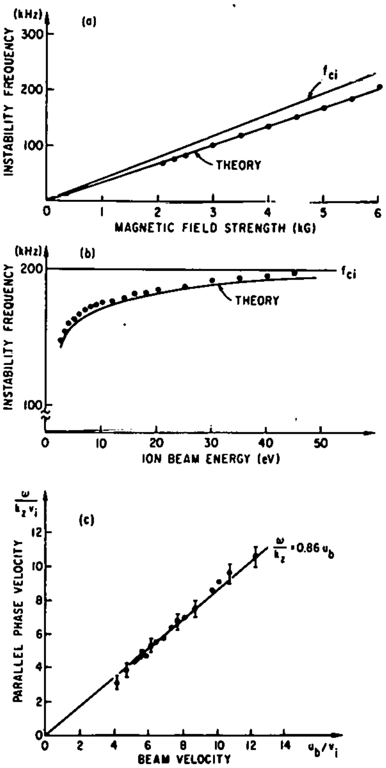

753942

Fig. 2. Instability Properties. (a) Frequency vs. magnetic field strength. $u_b = 7\times10^5$ cm/sec. (b) Frequency vs. ion beam energy. $u_t = (4T_o/m)^{1/2}$, i.e., sound velocity. In the calculation, $k_\perp\rho_i = 0.7 =$ const., experimentally $k_\perp\rho_i$ is 1.7 at onset and 0.7 far beyond onset, with 30% error. (c) Parallel phase velocity vs. beam velocity. Both axes normalized by $v_i = (2T_o/M)^{1/2}$.

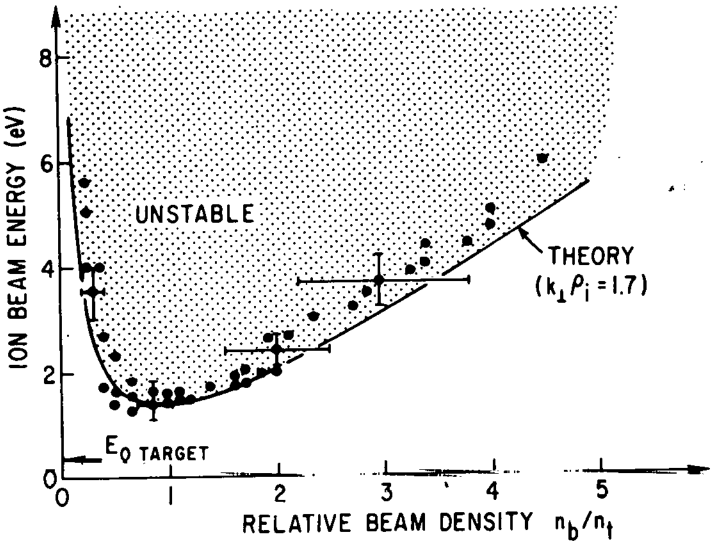

753931

Fig. 3. Threshold beam energy vs. relative beam density. The solid line was computed for the measured value of $k_\perp \rho_i = 1.7$, at onset.

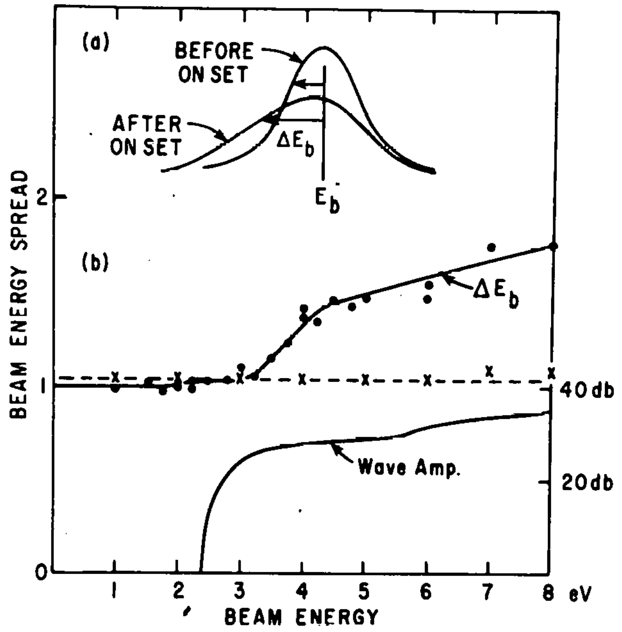

753943

Fig. 4. Beam energy spread with onset of instability. (a) Beam energy distribution before onset and with saturated instability. (b) Beam energy spread (normalized by the spread at E_b = 1 eV) and instability amplitude vs. beam energy. ● $n_b/n_t \simeq 2$, instability present; × $n_b/n_t \simeq 7$, instability absent.